

Enhancing Real-World Adversarial Patches with 3D Modeling Techniques

Yael Mathov, Lior Rokach, Yuval Elovici
Ben-Gurion University of the Negev, Israel

Abstract—Although many studies have examined adversarial examples in the real world, most of them relied on 2D photos of the attack scene; thus, the attacks proposed cannot address realistic environments with 3D objects or varied conditions. Studies that use 3D objects are limited, and in many cases, the real-world evaluation process is not replicable by other researchers, preventing others from reproducing the results. In this study, we present a framework that crafts an adversarial patch for an existing real-world scene. Our approach uses a 3D digital approximation of the scene as a simulation of the real world. With the ability to add and manipulate any element in the digital scene, our framework enables the attacker to improve the patch’s robustness in real-world settings. We use the framework to create a patch for an everyday scene and evaluate its performance using a novel evaluation process that ensures that our results are reproducible in both the digital space and the real world. Our evaluation results show that the framework can generate adversarial patches that are robust to different settings in the real world.

I. INTRODUCTION

The development of deep learning models has fostered solutions for challenges previously considered unsolvable. However, a concerning vulnerability in those models was discovered, where an imperceptible perturbation to a legitimate input sample creates an adversarial example that causes the model to output an incorrect prediction with high confidence [1]. Although adversarial examples were initially observed in the digital space [2], [3], they were later demonstrated in real life [4]. While several studies have presented various use cases for real-world adversarial examples in the image domain [5]–[7], they all utilized a similar methodology: First, one or more 2D photos of the target scene are used to craft an adversarial perturbation that can be digitally added to the entire image or applied as a patch to a portion of an image. Then, the perturbation is recreated in the real world (i.e., printed) and placed in the scene. Finally, photos of the manipulated scene are gathered and fed to the neural network for evaluation.

Although that methodology has shown promising results, Fig.1 demonstrates why 2D image-based methods are not suitable for the 3D real world. The main challenge stems from the fact that while both the photos of the scene and the adversarial perturbation are flat, the real-world scene is not. A flat patch must both be placed on a flat surface and always face the camera, otherwise parts of the patch will be hidden, and the attack can fail. Furthermore, crafting the perturbation based on photos of the scene limits the attacker’s ability to model real-world properties as part of the attack. Transformations to the scene, such as lighting, must be manually added to the real-

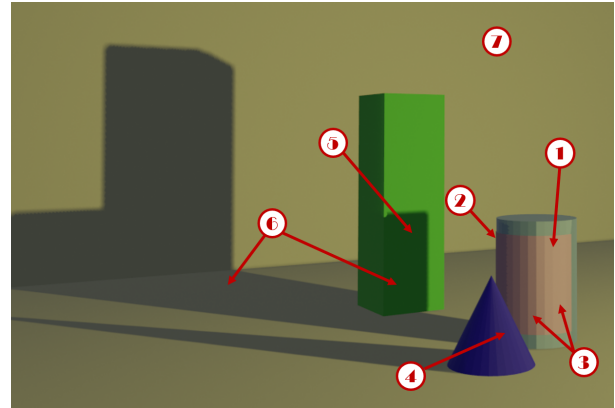


Fig. 1. Some of the challenges that should be addressed when crafting an adversarial patch for a real-world scene: 1) The patch is placed on a curved surface. 2) The patch is partially hidden by the object it is placed on. 3) The patch should have the same lighting as the rest of the scene. 4) The patch is hidden by an object that is placed in front of it. 5) Objects casting shadows on one another. 6) The scene includes an object that affects multiple objects. 7) The scene can have different lighting settings (i.e., point yellow light).

world scene, and only then can the attacker use them as part of the attack. However, such attacks can only be implemented when the attacker has full control of the target scene, which is a less realistic assumption.

Several studies focused on crafting adversarial perturbations for 3D objects. A prominent example is the expectation over transformation (EOT) framework [8] for crafting adversarial examples that are robust to random transformations (e.g., rotation, noise); the framework relies on the attacker’s ability to model those transformations as part of the attack process. In [8], EOT was used to perturb the texture of a digital 3D object, which was later printed using a color 3D printer. Although successful, the attack targeted a single object, as opposed to a complex scene containing several objects and other ambient elements. As Fig.1 shows, a realistic scene contains environmental characteristics (e.g., ambient lighting), and different objects that can affect one another (e.g., hide, shadow). Failing to consider those issues can impair the attack’s performance. Additionally, EOT relies on a specific implementation (limiting the ability to use external modeling and rendering tools) and the use of a 3D color printer, a piece of equipment which is not accessible to many people. Both issues complicate the attack and make it less feasible.

Another major issue of prior work in this area is the inability to perform the experiment in the real world multiple times

and obtain similar results. In some studies, it is impossible to perform the same real-world experiment more than once, limiting the ability to evaluate the attack. For instance, it is not possible to replicate and validate an experiment, in which a set of photos of the scene was obtained from random positions, if the exact positions are not documented by the authors. In other studies, the results cannot be replicated by other researchers, because the target scene or evaluation process cannot be (exactly) recreated by subsequent researchers. Thus, the scientific community cannot properly assess methods proposed in prior research on real-world adversarial examples.

In this paper, we present a framework that utilizes 3D computer graphic methods to craft adversarial patches that can be added to an existing real-life scene. Our approach allows the attacker to target complex realistic scenes, as well as to model and transform the scene’s objects, environmental characteristics, etc. The framework uses a digital 3D replica of the target scene to simulate the real world, thus allowing the attacker to assess the limitations of one the patch and improve it without risking detection. Since the attacker controls the digital replica, he/she can add, change, and remove different elements, and as a result can create a patch that is more robust to real-world transformations. The framework is designed to allow the integration of external modeling and rendering tools, which gives the attacker the flexibility to implement the attack using the tools he/she prefers. We implement the framework using open-source tools, and thus the attack is also accessible to an attacker with a limited budget.

In addition, we propose an evaluation process which is specifically designed so that the experiment can be replicated and performed multiple times. The two-step evaluation process is used in several experiments to evaluate our attack in both the digital space and the real world. We examine whether the use of a replica to create and improve an adversarial patch can simulate the patch’s performance in the real world. To do so, we use the framework to create adversarial patches of multiple target classes and use the evaluation process to compare their performance in digital space and the real world. Furthermore, in realistic settings, unexpected changes may occur in the target scene; therefore, we examine the patch’s robustness to changes in the scene that were not modeled as part of the scene’s replica. Therefore, we evaluate how changing or adding new objects to the scene affect the patch’s ability to fool the target neural network. By publishing our evaluation setup and code [9], researchers can reproduce our results and improve upon them.

The main contributions of this study are:

- We present a framework for crafting and improving adversarial patches for an existing real-world scene in the risk-free environment of the digital space.
- We demonstrate how the framework can be used to craft a low-budget adversarial patch using free, open-source, and common 3D modeling tools.
- We present an evaluation process that allows reproducible experiments in the digital space and the real world.

II. BACKGROUND

When discovered [1], adversarial examples were considered a minor “bug”; yet reality has changed with the development of advanced adversarial attacks and the growing number of failed attempts to defend against them [2], [3], [10]. Adversarial examples’ success at fooling neural networks led to interest in implementing attacks in the real-world [4]. However, the first real-world studies performed were unable to reproduce the results obtained in the digital space.

The initial studies did, however, set the stage for research aimed at creating adversarial patches [6], [11], which, when added to an image, can fool the classifier. In addition, the patch can be printed and placed in a real-world scene to achieve similar results. Similar techniques were used to create patches against object detectors [7], [12]. While the patches were crafted using EOT to improve their robustness to real-world transformations, in all cases, the patches were crafted in a 2D space but tested in a 3D space. As a result, the flat patch produced would be unable to address the real-world challenges presented in Fig.1. Therefore, there was a need to develop methods to improve attacks’ robustness in real-world settings.

A solution to those challenges emerged when the EOT framework [8] was used to craft perturbations that are robust to specific transformations. The framework builds a training dataset by transforming the original sample, using parameters that were randomly sampled from the transformation’s distribution. For example, to craft an adversarial example that is robust to rotation, the training set includes samples of the original image that are rotated at different angles. The framework was used to perturb the texture of a digital 3D object, which was later printed in the real world using a color 3D printer. However, the study focused on perturbing the texture of a single digital object and thus did not consider the challenges of a complex realistic scene (presented in Fig.1). While attackers aim to target an existing real-world scene, the EOT was demonstrated on an existing digital 3D object that was later printed in the real world. In addition, the implementation of the rendering process and the use of a color 3D printer complicate the attack.

While some studies examined how the representation of 3D data affects the model’s robustness to adversarial perturbations [13], others suggested methods for perturbing the structure (mesh) or texture of 3D objects [14], [15]. However, the methods focused on manipulating a single 3D object, thus failing to consider the special characteristics of a complex real-world scene. A more realistic approach is to perturb different realistic elements of a digital 3D scene [16] to gain more insights about attacks in the real world. Although using 3D objects to create realistic adversarial examples seems promising, the studies mentioned above use premade digital objects, do not target an existing complex real-world scene, and fail to examine the attack beyond the digital space.

The goal of our study is to use the techniques mentioned above to craft adversarial patches that are robust in real-world settings. We also improve upon previous research by allowing

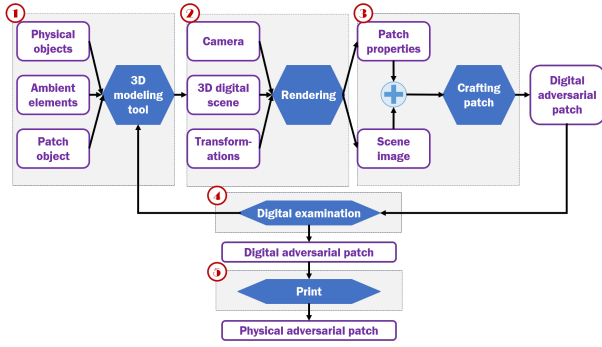


Fig. 2. The framework’s steps: 1) Model a digital replication for the real-world scene. 2) Render 2D images with realistic transformations. 3) Craft the adversarial patch. 4) Examine the adversarial patch in the digital space and improve the attack if needed. 5) Apply the patch to the physical scene.

the attacker to work in a flexible environment that simulates the real world. By creating a digital replica of the target scene, we give the attacker control of every element in the scene. Then, the attacker can effectively utilize EOT by transforming the digital scene to improve the perturbation’s robustness to the same transformations in real life.

III. SUGGESTED APPROACH

A. Assumptions and Threat Model

We assume an attacker that wants to add a simple patch to an existing real-world scene to “hide” an object from a deep learning-based system. By doing so, all photos of the scene will result in a false prediction by the target neural network. We assume the attacker has complete knowledge of the target neural network (e.g., parameters, architecture) but not of other components (e.g., camera). Moreover, the attacker can examine the real-world scene to create a 3D digital replica of it, such that the rendered images of the replica are classified by the neural network as the true class. Finally, we assume that the attacker has physical access to the real scene to add the patch in real life.

B. Framework Overview

We suggest the following framework for crafting an adversarial patch for an existing real-world scene. Fig.2 presents the five steps of the framework: model, render, craft, evaluate, and apply. The first four steps are performed in the digital space, while in the fifth step, the adversarial patch is transferred from the digital space to the real world.

First, the attacker creates a 3D digital replication of the real-world scene and adds an empty digital patch object to the replica. The texture of the empty object will be perturbed to craft the adversarial patch. Second, the digital replica is rendered into 2D images, such that each image is a rendering of the scene with real-world transformations (e.g., rotation, a change in the light color). For each image, the rendering process outputs a background image of the scene (without the patch) and the properties of the patch (all pixels that include the patch). This step allows the attacker to craft an adversarial patch without implementing a differentiable rendering

process or approximating the gradients of a non-differentiable rendering. Third, the attacker uses a differentiable method to combine the background and patch properties into one image to create a set of the scene’s images; this set is then used to perturb the patch’s texture, using any method for crafting an adversarial example. Fourth, the attacker adds the adversarial patch to the scene’s digital replica, renders images of the scene, and feeds them to the neural network. As a result, the attacker can examine the patch’s effect on the scene and improve it if needed. Finally, the attacker prints the final patch on a sticker and adds it to the real-world scene.

1) Modeling a Digital Replica of the Real-World Scene:

The first step is to create a 3D digital replica that approximates the target real-world scene. To build this replica, the attacker can choose any tool (e.g., Blender, Maya) and resources (e.g., make use of free 3D objects, buy 3D designs, use a 3D scanner) Then the attacker adds an empty 3D object to the digital scene for the adversarial patch. In this step, the attacker should consider the following elements: the objects in the scene, the ambient characteristics, and the adversarial patch. First, the replica is built from digital 3D objects that represent the objects in the real-world scene. Then, the scene’s ambient characteristics (e.g., light sources, shadows) are added to the replica to improve the replica’s similarity to the real world. Finally, the digital patch object is added to the scene, according to its expected location in real-life. The location, shape, and size of the patch should be determined based on the attacker’s goals and the camera’s expected location.

The modeling stage is affected by the expertise and resources of the attacker. Our findings show that a successful attack can be launched by roughly reproducing the target scene, however when more realistic replications are modeled, the success rate will likely increase. This allows a trade-off between the attacker’s effort and the success rate, which can be used to suit the goals and capabilities of the attacker.

2) Rendering 2D Images with Realistic Transformations:

The EOT process forms a collection of images with different transformations (“views”) and then crafts a single perturbation that fools the target neural network for all views. Unlike past studies that used EOT with a limited number of transformations, our framework’s design allows the attacker to transform any of the scene’s properties, including the scene’s objects (one or more), ambient characteristics, camera view, and more. As presented in [8], flexibility in choosing the transformations results in a better adversarial perturbation.

In this step, the attacker aims to create a collection of views, such that each view represents the digital replica under a set of transformations. To achieve this, the attacker chooses a list of scene transformations $T = \{T_1, \dots, T_k\}$ and camera transformations C . Then, given the 3D digital replica S with patch texture P , the attacker builds a collection of views X :

$$X = \mathbb{E}_{t \sim T, c \sim C} [R(S, P, t, c)]$$

where R is a rendering process that creates 2D images of the 3D scene with the t transformations from viewpoint c .

Most optimization problems for crafting adversarial perturbations are solved by calculating or approximating the attack’s loss gradient concerning the patch. However, crafting X uses an external rendering process R , which can be non-differentiable, thus preventing the attacker from calculating $\frac{\partial X}{\partial P}$. Past studies overcame this challenge by implementing the rendering process as part of the attack [8], [14] or by approximating the loss gradient [15], [16]. However, these solutions prevent the attacker from using external tools and increase the knowledge required to implement an attack. Therefore, we suggest splitting the rendering output into two parts: the background and the patch’s properties. The background is an image of the scene without the patch, and the patch’s properties form a set of buffers with information that allows the patch to be added to the background in a realistic manner; combining the two creates an image of the scene.

3) *Crafting the Adversarial Patch*: The rendering stage results in a collection $X = \{(b_i, p_i)\}_{i=1}^n$, where for sample i , b_i is the scene background, and p_i is the patch properties. Given a sample i , let $B(P, b_i, p_i)$ be a differentiable method that combines the patch’s texture P , the scene’s background, and the patch’s properties in the image of the rendered scene. For most patch properties, implementing B can be easily achieved using a sequence of add and multiply operators. The attacker builds a set of views \tilde{X} based on X :

$$\tilde{X} = \{B(P, b_i, p_i) : \forall (b_i, p_i) \in X\}$$

Then, the attacker perturbs P to fool a neural network M , by optimizing an objective function with a customized attack loss \mathcal{L} , such as $\arg \min_P (\mathcal{L}(M(\tilde{X})))$. The attacker can construct \mathcal{L} to create a targeted attack, apply constraints, etc. The objective function and optimization method should be selected according to the attack’s goal and target neural network.

4) *Examining the Patch in the Digital Space*: Next, by adding the patch to the digital replica, the attacker can simulate the adversarial patch’s effect on the neural network’s prediction concerning the real-life scene. Examining the adversarial patch in the real-world requires the attacker’s presence at the original scene and performing actions there that could be considered abnormal, thus exposing the attacker to the risk of detection. Therefore, the ability to use the digital replica to simulate the real-world scene allows the attacker to identify problems and improve the patch in a controlled and safe environment. The attacker controls the digital replica and therefore can simulate events that are challenging to control in real life (e.g., waning daylight, the presence of smoke, etc.) Moreover, the replica allows the attacker to compare different adversarial patches to identify the most effective one and improve the attack’s success in the real world. Based on this, the attacker might want to change the attack process, requiring modifications to the scene’s replica, the addition of new transformations to the rendering step, or changes to the attack’s optimization function. Since all of these are performed in the digital space, the process of improving and evaluating the patch can continue as long as the attacker wishes.

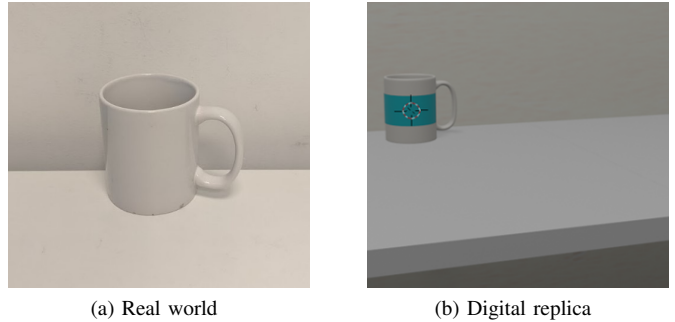


Fig. 3. The target scene: a white mug placed on an office desk; (a) is a photo of the original real-world scene, and (b) is a rendering of our digital replica with the empty adversarial patch (blue strip) that was modeled using Blender.

5) *Applying the Patch to the Physical Scene*: Finally, the attacker can create an adversarial patch in real life and add it to the scene. The patch can be printed on a sticker or even on a piece of paper, using a home printer.

IV. EXPERIMENTAL SETUP

In this study, we implement the framework using free and open-source software, to create an adversarial patch for a typical office scene in which a common white mug is placed on a desk, as seen in Fig.3a. A webcam (Microsoft LifeCam VX-700) films the scene, and we divide the video stream into photos, and crop and feed them to the object classifier (InceptionV3 [17]). This classifier was trained on the ImageNet dataset [18], achieving 1-top accuracy of 78% and 5-top accuracy of 93.9% for valid input. We validated that the scene is classified as the Coffee Mug class 100% of the time. Additional information on the experiment, code, and parameters is available at [9].

A. Crafting the Adversarial Patch

1) *Modeling*: To model the replica of the target scene, we use the free creation software Blender [19]. We start by approximating the objects in the real-world scene; for the room and desk, we can use default shapes that exist in Blender, but modeling the mug is more complex. Therefore, we use a free, pre-made mug object [20] and add it to the digital replica. Then, we add a yellow light source that simulates the light bulb in the original office. To create the empty adversarial patch, we crop and edit parts of the mug’s model [20] and add it to the digital scene. For each object, we choose common configurations for the materials and textures that are made from photos of the real-world scene. We note that the replica is modeled using online tutorials for beginners, to serve as a simple approximation of the real-world scene. Therefore, while our digital scene lacks some realistic elements (Fig.3b), it can be easily replicated by researchers with limited experience in 3D modeling.

2) *Rendering*: The rendering is implemented with ModernGL [21], based on the examples in the library’s repository, and uses the configurations and materials to portray the

ambient elements in the rendered images (e.g., shadows). We render a set of views, i.e., images from the scene with different transformations. For the transformations, we choose translation and rotation in the x, y , and z axes, and changes in the light color and camera’s position. Each transformation’s range is defined according to possible changes in the real-life scene and ensures that the mug is visible in all views. Due to the attacker’s assumed lack of knowledge about the camera, we estimate the camera’s configurations (available at [9]).

We explore two methods for sampling the parameters for the transformations: random and systematic. Random sampling is commonly used in the EOT framework; for transformation T_i the parameters are randomly sampled from a range $[\alpha_i, \beta_i]$ (i.e., $T_i \sim U(\alpha_i, \beta_i)$). Additionally, we examine a deterministic approach, which we refer to as systematic sampling, where for each transformation T_i , the parameters are sampled in constant even steps across $[\alpha_i, \beta_i]$. Hence, sampling l parameters for T_i will result in the same set of values: $\{\alpha_i + \frac{j \cdot (\beta_i - \alpha_i)}{l}\}_{j=0}^l$. Then, to build the image set, we render an image of the scene for every combination of those parameters for the different transformations. The set of views is rendered based on the sampled parameters (using one of the sampling methods); for each view, the rendering process outputs four buffers: a background image and three buffers with the patch information.

3) *Crafting*: For both sampling methods, we use a sequence of add and multiply operations to build a set of images \tilde{X} out of a set of views X and the patch’s texture P , such that calculating $\frac{\partial \tilde{X}}{\partial P}$ is trivial. Then, we use the Adam optimizer to find an adversarial perturbation for P based on:

$$\arg \min_P \{CE(\tilde{X}, y_{target}) - \kappa \cdot CE(\tilde{X}, y_{true}) + \lambda \cdot TV(P)\}$$

where κ, λ are tuning parameters, and y_{true}, y_{target} are the true and attack target class respectively, CE is the cross-entropy loss, and TV is the total variation.

4) *Examination*: To examine the patch, we use the digital evaluation process which is described in Sec. IV-B. Our main tweaks are aimed at improving the replica (e.g., creating a realistic lighting by modeling the room as a box instead of the three visible walls) and changing the transformation ranges. The attack was initially designed for the Armadillo target class; later, we change the seed and initialization parameters and use the attack to craft patches for the Armadillo and nine additional target classes. We use the same attack to perform a non-biased comparison between the patches, however a more realistic approach would be to build a tailored attack for each target class.

5) *Application*: We print the patch on an A4 piece of paper using a Xerox WorkCentre 6605, crop it, and apply it to the mug using transparent adhesive tape.

B. Evaluation Process

Performing the same experiment multiple times under the same conditions and obtaining similar results is important for both our study’s integrity and to support future work.

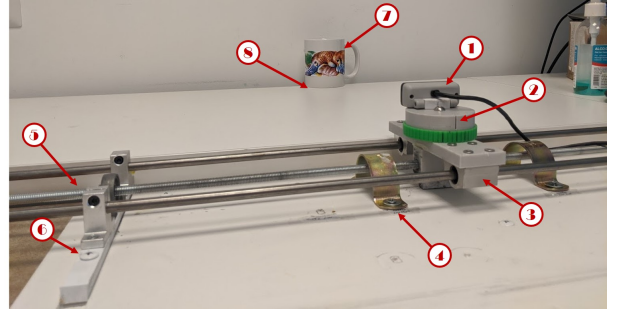


Fig. 4. Our real-world evaluation setup: The position of the camera (1) is controlled by spinning a platform with gradations at its base (2). The platform is located on a cart (3), which moves within predefined ranges (4) on a spinning screw rod (5). The slider can be moved forward and backward into one of three predefined positions (6). We can rebuild the scene using the markings for the mug’s location and position (7), and the patch’s location on the mug (8).

Therefore, we suggest a replicable two-step evaluation process, the first step of which takes place in the digital space; the second step takes place in the real world. We note that the evaluation process was designed for research purposes and is not part of the framework.

1) *Digital Space*: At the first step, the digital replica is used to simulate the evaluation in the real world, similarly to our framework’s examination step (step 4 in Fig.2). Here, we add the adversarial patch to the scene, render a set of images under the expected real-world settings and transformations (e.g., camera’s location or position), send the images to the neural network, and analyze the predictions.

2) *Real-World*: To ensure that the real-world evaluation process is reproducible, we suggest building a camera slider, as presented in Fig.4. A camera is placed on a spinning platform, which is located on top of a cart used to place the camera in front of the scene. The position of the camera can be changed by spinning the platform at a predefined angle and then securing it in-place with a screw. Since the base of the platform has gradations, a specific position can be marked on the base for later use. A motor spins a screw rod, which moves the cart across two metal rods at a constant speed. We suggest defining small ranges along the slider, from which the scene is filmed at different angles. For example, by changing the camera’s position, small ranges of the scene can be filmed (from the center and from the left and right of the slider) to ensure that we are only filming relevant areas of the scene (i.e., areas where the mug is visible). The ranges can be set by physically limiting the cart’s movement or by reconfiguring the motor’s behavior. Additionally, the slider can be moved forward and backward across a grooved base to film the scene from different distances. Finally, since the real world scene might change, the location and position of each object, including the adversarial patch, must be marked, thus ensuring that the same scene can be evaluated again. By physically marking each configuration, the same actions can be performed in future experiments and thus, achieve similar results.

3) *Our Evaluation Setup*: Implementation available at [9].

Digital space: We determine 3,360 different positions and locations for the camera around the object, based on the patch’s visibility in the digital replica; for each of them, we render an image and send it to the object classifier. Since a similar evaluation process was used to configure our attack, we craft and perform the evaluation on a set of unseen patches.

Real world: We build the structure, as shown in Fig.4 and described above. The slider can be placed at one of three predefined distances from the scene (close, middle, and far). For each distance, we predefined three ranges (left, center, and right), and set each of the nine ranges with metal eye straps. The location of mug, the position of the mug’s handle, and the place of the patch on the mug are marked, thus ensuring that the same scene is used throughout the various experiments.

V. RESULTS

For each target class, we craft four patches: *random*, *systematic*, *google*, and *imagenet*. The *random* and *systematic* patches are adversarial patches crafted by using our framework with random or systematic sampling of the transformations. The *google* and *imagenet* patches are made out of images of the target class that were obtained from a Google search or the ImageNet dataset respectively, and are used to ensure that the results are non-biased. We note that the images used for the *imagenet* patches were collected from the dataset that was used to train the classifier, Inception V3. We also examine the classification results for a mug without a patch (*clean*) and a patch with random pixel values (*noise*). For each target class and its four patches, we evaluate the percentage of images that are classified as the true class (Coffee Mug), target class, or other classes (out of the ImageNet dataset).

A. Results for Evaluation in the Digital Space

After changing the seed and initialization parameters, we craft *random*, *systematic*, *google*, and *imagenet* patches for the following classes: Armadillo, Hat, Nipple (bottle), Platypus, Mask, Pencil Box, Syringe, Screw, Mousetrap, and Ladybug. Then, we performed the evaluation process in the digital space for *clean*, *noise*, and for each of the described patches. All of the 3,360 images are classified as the true class, Coffee Mug, for *clean* and the *noise* patch; Table I summarizes the results for the remaining patches.

We expected that the *imagenet* patches, which were taken from the dataset that was used to train Inception V3, would act like an adversarial patch, thus causing the scene to be classified as the target class. Yet, although the scene is simple, the *google* and *imagenet* patches, with clear images of the target class, do not affect the classifier. On average, 99% of the rendered images of the replica with the *google* and *imagenet* patches are classified as the true class, and none of them are classified as the target class; while more than 99% and 97% (on average) of the images are classified as the target class for the *systematic* and *random* patches respectively. When comparing the two types of adversarial patches, the systematic sampling approach is significantly (p-value is 0.04 for a paired sample t-test) better

at causing the scene to be classified as the target class than the random sampling approach.

B. Results for Evaluation in the Real World

For the real-world evaluation, we use the same patches we created in the digital space for the following target classes: Armadillo, Hat, Nipple, and Platypus. Each patch, including the *noise* patch, is printed on a piece of paper, cropped, and placed at the designated location on the coffee mug using a transparent adhesive tape. Then, we follow the setup presented in Fig.4 to film approximately 700 photos, for nine ranges of the real-world scene with each patch and *clean*. Similarly to the evaluation in the digital space, 100% of the photos of the real-world scene for *clean* and the *noise* patch are classified as the true classes; and Table II summarize the results for the remaining patches.

The results for the real-world evaluation are similar to the results obtained in the digital space. For all target classes, the scene with the *google* and *imagenet* is mainly classified as the true class (for 98.5% of the photos on average) and is never classified as the target class. Similarly, the scene with the adversarial patches *systematic* and *random* is mainly classified as the target class; the average difference between the digital and real-world results is 5%, and never exceeds 7%. We then examine the patches with a large difference between the results in the digital space and real world. The *google* patch for the Armadillo target class and the *imagenet* patch for Hat are classified as the true class in 98.1% and 99.1% of the images, but only in 95.8% and 95.9% of the photos of the real-world scene. Both patches are classified as the Candle class from the ImageNet dataset (other) for photos taken from positions in which the mug’s handle is less visible; therefore, the misclassification might stem from the cylindrical shape of the mug without the handle. We also observe that the *random* patch for the Platypus class is less effective when the camera is located far from the scene, in both the digital space and the real world. Since the digital space evaluation reveals its weaknesses, the attacker can utilize this information to improve the patch by rendering more views in which the camera is located far from the scene. This is an example of how the attacker can identify the patch’s flaws in advance, learn how to improve it, and increase the chances of a successful attack.

VI. RESILIENCE TO UNEXPECTED TRANSFORMATIONS

In realistic scenarios, the attacker cannot control the real-world scene, which means that by the time the attacker returns to the scene with the patch, the scene may have changed. As we discussed, the attacker can use our framework to improve the patch’s robustness to predictable changes, yet this is not the case for unexpected major transformations to the scene, (e.g., removal of an object, changes in the objects’ location). If the patch is only effective in the modeled scene and under expected transformations, then our framework is less feasible in real-world settings. Therefore, we want to understand how unexpected transformations to the real-world scene affect the

Target Class	Systematic			Random			Google			Imagenet		
	%True	%Target	%Other	%True	%Target	%Other	%True	%Target	%Other	%True	%Target	%Other
Armadillo	0.3	99.5	0.2	0.8	98.5	0.7	98.1	0	1.9	98	0	2
Hat	0.3	99.6	0.1	0.1	99.5	0.4	99.5	0	0.5	99.1	0	0.9
Nipple	0.1	97.6	2.3	0.4	93.1	6.5	99.6	0	0.4	100	0	0
Platypus	1	97.5	1.5	1.3	98	0.7	98.1	0	1.9	96.4	0	3.6
Mask	1	99	0	6.9	92.9	0.2	99.7	0	0.3	99.7	0	0.3
Pencil Box	0	99.9	0.1	0.7	98.7	0.6	99.7	0	0.3	99.9	0	0.1
Syringe	0	98.9	1.1	0.8	95	4.2	99.2	0	0.8	97.6	0	2.4
Screw	0.1	99.8	0.1	0.6	97.6	1.8	100	0	0	97.9	0	2.1
Mousetrap	0	100	0	0.1	99.1	0	100	0	0	97.9	0	2.1
Ladybug	0	100	0	0	100	0	99.7	0	0.3	100	0	0

TABLE I

THE CLASSIFICATION RESULTS (PERCENTAGE) IN THE DIGITAL SPACE. ALL OF THE IMAGES ARE CLASSIFIED AS THE TRUE CLASS FOR *clean* AND *noise*.

Target Class	Systematic			Random			Google			Imagenet		
	%True	%Target	%Other	%True	%Target	%Other	%True	%Target	%Other	%True	%Target	%Other
Armadillo	1.5	92.8	5.7	2.1	95.3	2.6	95.8	0	4.2	99.7	0	0.3
Hat	0	99.1	0.9	0.2	98.9	0.9	99.3	0	0.7	95.9	0	4.1
Nipple	0	98.7	1.3	0.7	92.7	6.6	100	0	0	99.1	0	0.9
Platypus	0.3	92.6	7.1	6.2	87	6.8	99.2	0	0.8	99.1	0	0.9

TABLE II

THE CLASSIFICATION RESULTS (PERCENTAGE) IN THE REAL WORLD. ALL PHOTOS ARE CLASSIFIED AS THE TRUE CLASS FOR *clean* AND *noise*.

ability of adversarial patches created using our framework to fool the target neural network. To do so, we change the real-world scene, by using seven new transformations. The adversarial patches are not expected to be robust to those transformations, since they do not appear as part of the replica.

As shown in Fig.3a, the original scene contains a white coffee mug with a handle on the right side and a patch placed in the middle of the mug, which is placed on an office desk. We defined the seven unexpected transformations as *up*, *down*, *red*, *wood*, *color*, *shape*, and *flipped*. *Up* and *down* are transformations to the patch’s location on the mug; the patch is placed on the top and bottom of the mug respectively. We also change the surface on which the mug is placed to a red circle (*red*) and a wooden mat (*wood*). For *color* and *shape*, we replace the original white mug: for *color*, we use a mug of the same shape but with a different color (a dark background with illustrations), while for *shape*, we use a mug of a similar color (light gray) which has a different shape. The *shape* mug is shorter and cone-shaped, and has a smaller handle which is located at a higher position on the mug. Finally, for *flipped*, we rotate the mug by 180°. In this experiment, for each transformation (some of these are shown in Fig.5) we change the scene and perform the real-world evaluation process with the two adversarial patches (*systematic* and *random*) used for the Nipple target class. Table III presents how each unexpected transformation affects the classification results of the real-world scene with the adversarial patches.

The unexpected transformations cause the scene to be classified less often as the target class and more often as other; yet the scene is classified as the true class in only 2.9% of the photos on average (and in no more than 6.5% of the photos). Thus, the neural network fails to identify the mug even when there are major unexpected changes in the scene. It seems that



(a) Different mugs

(b) Red mat

Fig. 5. Unexpected transformations to the real-world scene; (a) shows the three coffee mugs on the wooden mat used for *wood* (from left to right: *shape*, the original mug, and *color*), and (b) is a picture of *red*: the original coffee mug with an adversarial patch on a red mat.

Transformation	Systematic			Random		
	True	Target	Other	True	Target	Other
Up	0.6	88.9	10.5	2.2	77.9	19.9
Down	2.7	83.7	13.6	2.7	87.8	9.5
Red	1.9	84.6	13.5	2.7	76.5	20.8
Wood	5.8	68.9	25.3	2.4	64.7	32.9
Color	6.5	39.1	54.4	5.5	28.1	66.4
Shape	0	87.1	12.9	1.2	71.7	27.1
Flipped	2.7	85.8	11.5	4.3	55.1	40.6

TABLE III

THE RESULTS OF A REAL-WORLD EVALUATION FOR THE NIPPLE PATCHES WITH SEVEN UNEXPECTED TRANSFORMATIONS ADDED TO THE SCENE.

THE RESULTS INDICATE THE PERCENTAGE OF PHOTOS THAT WERE CLASSIFIED AS THE TRUE, TARGET, OR OTHER CLASSES.

the patches are robust to changes in the patch’s location on the mug; in this case, the scene is classified as the true class for no more than 2.7% of the photos. However, changes in the object that the mug is placed on show mixed results; while the patches are more robust to *red*, *wood* is classified as the target class in less than 70% of the photos, and in up to 5.8% of the photos as the true class. We believe that the difference

may stem from the shape of the mats: unlike the wooden mat, the red mat and the desk in the original scene have a solid shape. Similarly, replacing the original mug also shows mixed results; both patches perform the worst on *color* but perform well on *shape*. For *color*, the scene is classified as the target class in less than 40% of the photos and as the true class in up to 6.5% of the photos. We assume that the use of a mug with an inconsistent design (i.e., many illustrations) reduces the robustness of the patches. Although the patches are the least robust to *color*, the neural network still fails to identify the scene in more than 90% of the photos. In contrast, the scene with *shape* is classified as the target scene in 71.7% and 87.1% of the photos for the *random* and *systematic* patches respectively, and the *systematic* patch is never classified as the true class. Additionally, we find that *flipped* affects the adversarial patches differently: *systematic* performs well, with 85.8% of the photos classified as the target class, but for *random* only 55.1% of the photos are classified as the target class. Finally, in most cases, the *systematic* patch performs better than the *random* patch.

This experiment is designed to examine whether using a digital replica limits the attack to a specific model of the scene, thus causing the adversarial patch to become ineffective when unexpected changes occur in the real world. To do so, we perform noticeable, yet realistic, transformations to the original real-world scene: changes in an object’s location and position, the replacement of an object, and adding a new object to the scene. The results show that although the transformations reduce the attacker’s ability to control the neural network prediction, the patches are still able to fool the neural network so that it misclassifies the scene. On average, the scene is not classified as the true label in more than 97% of the photos, which supports the feasibility of our framework. Therefore, the attacker can improve the attack’s robustness to real-world transformations by creating a 3D replica of the scene, suffering just a minor reduction in the patch’s fooling ability if unexpected changes occur in the scene.

VII. CONCLUSIONS

In this work, we demonstrated how 3D modeling and rendering tools can be used to craft inexpensive adversarial patches that are robust to real-world transformations. By creating a digital replica of the target scene, our method gives the attacker control of every aspect of the scene, including the objects, lighting, and more. The replica simulates the real-world scene, thus allowing the attacker to test and improve the attack without the risk of detection. We also demonstrate that such flexibility can improve the patch’s robustness to both expected and unexpected changes in the real-world scene. Additionally, we present an evaluation process that enables other researchers to reproduce our experiments and validate our results. We believe that such an evaluation process can be used in future studies and contribute to the ability to replicate, examine, and improve other real-world attacks.

In future work, we plan to improve the suggested framework by adding 3D elements (e.g., reflection and normal maps) to

support more complex scenes. Then, we will use it to tailor an attack for other domains, like the facial recognition domain, where our framework can be used to improve individuals’ privacy with respect to such systems. We also aim to create imperceptible perturbations that attract less attention. Finally, our results suggest that using the EOT framework with systematic sampling might be better than random sampling, however additional experiments are needed to verify this observation.

ACKNOWLEDGMENT

A grateful acknowledge to Matan Yesharim for his major contribution to the development of both the attack and evaluation frameworks. We also thank Boris Zadov for his professional expertise. Finally, a special thanks to Mathov Designs for designing and building the real-world evaluation framework; we thank you for allowing us to publish your designs which will assist the research community around the world.

REFERENCES

- [1] C. Szegedy, W. Zaremba, I. Sutskever, J. Bruna, D. Erhan, I. Goodfellow, and R. Fergus, “Intriguing properties of neural networks,” *arXiv preprint arXiv:1312.6199*, 2013.
- [2] I. J. Goodfellow, J. Shlens, and C. Szegedy, “Explaining and harnessing adversarial examples,” *arXiv preprint arXiv:1412.6572*, 2014.
- [3] N. Papernot, P. McDaniel, S. Jha, M. Fredrikson, Z. B. Celik, and A. Swami, “The limitations of deep learning in adversarial settings,” in *2016 IEEE European symposium on security and privacy (EuroS&P)*. IEEE, 2016, pp. 372–387.
- [4] A. Kurakin, I. Goodfellow, and S. Bengio, “Adversarial examples in the physical world,” *arXiv preprint arXiv:1607.02533*, 2016.
- [5] M. Sharif, S. Bhagavatula, L. Bauer, and M. K. Reiter, “Accessorize to a crime: Real and stealthy attacks on state-of-the-art face recognition,” in *Proceedings of the 2016 ACM SIGSAC conference on computer and communications security*, 2016, pp. 1528–1540.
- [6] I. Evtimov, K. Eykholt, E. Fernandes, T. Kohno, B. Li, A. Prakash, A. Rahmati, and D. Song, “Robust physical-world attacks on deep learning models,” *arXiv preprint arXiv:1707.08945*, 2017.
- [7] M. Lee and Z. Kolter, “On physical adversarial patches for object detection,” *arXiv preprint arXiv:1906.11897*, 2019.
- [8] A. Athalye, L. Engstrom, A. Ilyas, and K. Kwok, “Synthesizing robust adversarial examples,” in *International conference on machine learning*. PMLR, 2018, pp. 284–293.
- [9] Y. Mathov, “Enhancing real-world adversarial patches with 3d modeling techniques.” [Online]. Available: <https://github.com/yaliMa/Adversarial-Patch-3D>
- [10] N. Carlini and D. Wagner, “Towards evaluating the robustness of neural networks,” in *2017 IEEE Symposium on Security and Privacy (SP)*. IEEE, 2017, pp. 39–57.
- [11] T. Brown, D. Mane, A. Roy, M. Abadi, and J. Gilmer, “Adversarial patch,” 2017.
- [12] X. Liu, H. Yang, Z. Liu, L. Song, H. Li, and Y. Chen, “Dpatch: An adversarial patch attack on object detectors,” *arXiv preprint arXiv:1806.02299*, 2018.
- [13] J.-C. Su, M. Gadelha, R. Wang, and S. Maji, “A deeper look at 3d shape classifiers,” in *Proceedings of the European Conference on Computer Vision (ECCV)*, 2018, pp. 0–0.
- [14] C. Xiang, C. R. Qi, and B. Li, “Generating 3d adversarial point clouds,” in *Proceedings of the IEEE/CVF Conference on Computer Vision and Pattern Recognition (CVPR)*, June 2019.
- [15] C. Xiao, D. Yang, B. Li, J. Deng, and M. Liu, “Meshadv: Adversarial meshes for visual recognition,” in *Proceedings of the IEEE Conference on Computer Vision and Pattern Recognition*, 2019, pp. 6898–6907.
- [16] X. Zeng, C. Liu, Y.-S. Wang, W. Qiu, L. Xie, Y.-W. Tai, C.-K. Tang, and A. L. Yuille, “Adversarial attacks beyond the image space,” in *Proceedings of the IEEE Conference on Computer Vision and Pattern Recognition*, 2019, pp. 4302–4311.

- [17] X. Xia, C. Xu, and B. Nan, "Inception-v3 for flower classification," in *2017 2nd International Conference on Image, Vision and Computing (ICIVC)*. IEEE, 2017, pp. 783–787.
- [18] J. Deng, W. Dong, R. Socher, L.-J. Li, K. Li, and L. Fei-Fei, "Imagenet: A large-scale hierarchical image database," in *2009 IEEE conference on computer vision and pattern recognition*. Ieee, 2009, pp. 248–255.
- [19] B. O. Community, *Blender - a 3D modelling and rendering package*, Blender Foundation, Stichting Blender Foundation, Amsterdam, 2018. [Online]. Available: <http://www.blender.org>
- [20] SEED.EA, "Pica pica - seed coffee mug," 2018. [Online]. Available: <https://www.ea.com/seed/news/seed-project-picapica>
- [21] S. Dombi, SimLeek, Aljenci, MinchinWeb, Silxstudio, stuaxo, T. Aarnio, J. Reibert, E. Forselv, and J. Hartley, "Moderngl," 2018. [Online]. Available: <https://github.com/moderngl/moderngl>